

Directional direct detection of light dark matter up-scattered by cosmic-rays from direction of the Galactic center

Keiko I. Nagao^{a,1} Satoshi Higashino^{b,2} Tatsuhiro Naka^{c,3}
Kentaro Miuchi^{c,4}

^aDepartment of Physics, Okayama University of Science, Okayama, 700-0005, Japan.

^bDepartment of Physics, Kobe University, Hyogo 657-8501, Japan.

^cDepartment of Physics, Toho University, Chiba 274-8510, Japan.

E-mail: nagao@ous.ac.jp, higashino@people.kobe-u.ac.jp,
tatsuhiro.naka@sci.toho-u.ac.jp, miuchi@phys.sci.kobe-u.ac.jp

Abstract. Dark matters with MeV- or keV-scale mass are difficult to detect with standard direct search detectors. However, they can be searched for by considering the up-scattering of kinetic energies by cosmic-rays. Since dark matter density is higher in the central region of the Galaxy, the up-scattered dark matter will arrive at Earth from the direction of the Galactic center. Once the dark matter is detected, we can expect to recognize this feature by directional direct detection experiments. In this study, we simulate the nuclear recoils of the up-scattered dark matter and quantitatively reveal that a large amount of this type of dark matter is arriving from the direction of the Galactic center. Also, we have shown that the characteristic signatures of the up-scattered dark matter can be verified with more than 5σ confidence levels in the case of all assumed target atoms in the scope of the future upgrade of the directional detectors.

Contents

1	Introduction	1
2	CR-DM and the density profile	2
3	Numerical Result and discussion	3
3.1	Angular distribution of CR-DM and nuclear recoil	3
3.2	Energy dependence of the angular distribution	4
3.3	Asymmetry and sensitivity	5
4	Conclusion	7
A	The SI and SD cross section	13

1 Introduction

The identity of dark matter (DM) is a highly significant question in cosmology and particle physics. In the past a few decades, the weakly interacting massive particles (WIMPs) have been expected to be the identity of DM, and a lot of attempts have been made to detect them directly and indirectly, and to produce them in collider experiments. However, despite advances in the sensitivity of direct detection experiments, no obvious detection of DM has been achieved so far. Particularly, direct detection experiments have placed very stringent limits on the magnitude of the interaction cross section for WIMP particles of GeV-scale mass, i.e. $\sigma_{\text{SI}} < 6.5 \times 10^{-48} \text{ cm}^2$ and $\sigma_{\text{SD}} < 3.1 \times 10^{-41} \text{ cm}^2$, where $\sigma_{\text{SI(SD)}}$ represents spin-independent (SI) and spin-dependent (SD) cross section of the DM and proton scattering, respectively [1, 2]. On the other hand, for DM having lighter mass than GeV-scale, it is not easy to obtain high sensitivity through DM-nucleon scatterings. It has recently been proposed that even in such light DM cases, unavoidable scattering of DM and cosmic-ray produces substantial and very energetic DM that can be detected in the neutrino detectors and direct detection experiments of DM [3–12]. As well as the up-scattering of DM by cosmic-rays, its effect to cosmic-ray propagation in the Earth [3] has also been investigated. The cosmic-ray scattered dark matter (CR-DM) flux has a substantial contribution from the direction of the Galactic center.

Directional direct detection of DM is expected to be very well suited to detect the characteristic event of CR-DM coming from the Galactic center. This study simulates the CR-DM signals in directional searches and reveals its potential for validation against CR-DM. In directional detection, gas detectors are sensitive to the SD interaction of DM and nucleon [13, 14]. The gases used in the experiments are CF_4 and SF_6 , and in most of the cases, the target for scattering with DM is fluorine (F). In this paper, we also investigate a solid detector NEWSdm [15, 16], which is nuclear emulsion detector and is sensitive to the SI interaction. Nuclear emulsion detectors contain multiple targets, and in the numerical calculations, hydrogen (p), which is sensitive to light DM, and silver (Ag), which is sensitive to heavy DM, are employed as targets.

The rest of this paper is organized as follows. Section 2 introduces the method of CR-DM simulation and the DM profiles assumed in the simulation. Section 3 presents numerical results and discusses the detectability. Finally, we conclude the paper in Section 4.

2 CR-DM and the density profile

In order to simulate the scattering of CR-DM and targets in direct detection experiments, first the flux of incoming CR-DM to the earth is required. In this section, we basically follow the method of reference [4] to find the arriving CR-DM from each direction of the space. The calculation procedure is described below in order.

1). Once we assume DM mass m_χ , the interaction cross section $\sigma_{\chi i}$ between DM and nucleus i , density profile $\rho_\chi(r)$, and cosmic-ray flux $d\Phi_i/dT_i$ in the Galaxy, the CR-DM flux can be obtained by

$$\frac{d\Phi_\chi}{dT_\chi d\Omega} = \int_{l.o.s.} l^2 dl \frac{1}{4\pi l^2} \sigma_{\chi i} \frac{\rho_\chi(r)}{m_\chi} \frac{d\Phi_i}{dT_i}, \quad (2.1)$$

where l and r are the length of the line-of-sight (l.o.s) integral and the distance from the Galactic center, respectively, and T_χ and T_i are the kinetic energies of the CR-DM and nucleus, respectively. Hydrogen, which is the most abundant in space, is assumed as cosmic-ray particle i , i.e., we assume $i = p$ for simplicity in this paper.

To define the direction of the incoming CR-DM and the nuclear recoil, the coordinate system shown in Figure 1 is adopted. We define the direction of incoming CR-DM with θ_{DM} and ϕ_{DM} , and the direction of nuclear recoil as θ_N and ϕ_N , respectively. Note that in this case, $\theta_{DM} = \phi_{DM} = 0$ corresponds to events arriving from the direction of the Galactic center. The scattering angle $\gamma_{G.C.}$ is the angle from the line connecting the Galactic center and the observer. It is apparent that there is a relation $\cos \gamma_{G.C.} = \cos \theta_N \cos \phi_N$ between θ_N, ϕ_N and $\gamma_{G.C.}$. To include contributions near the Galactic center to the integration for l , the integration range is taken up to the distance between the solar system and the Galactic center, $d = 8$ kpc.

The cosmic-ray flux data from Galprop code [17] are used in the numerical calculation. Cosmic-ray sources would be denser in the vicinity of the Galactic center as well as the DM profile in a realistic scenario; however, following the paper [4] we assume that the flux of cosmic rays is uniform throughout the Galaxy.

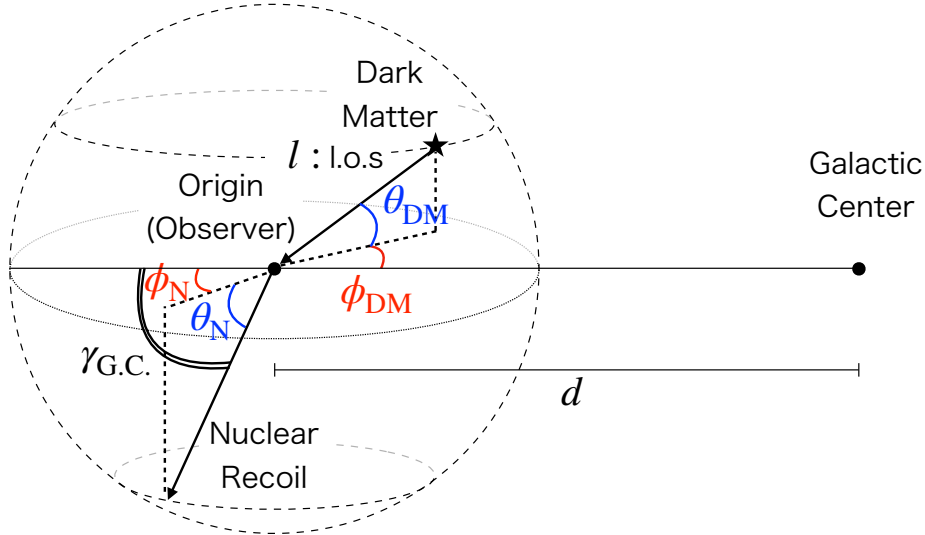


Figure 1: Coordinate system used in the figures showing the numerical results.

2). The obtained CR-DM flux in the Galactic rest frame is converted to that in the laboratory system on the Solar system.

3). DM-nucleon scattering caused by the CR-DM in the Solar system is simulated using the CR-DM flux derived by step 2). The nuclear recoil energy E_R and its scattering angle $\gamma_{\text{G.C.}}$ are obtained.

As the density profile $\rho_\chi(r)$, three typical profiles are assumed. The first one is the most commonly used, the Navarro–Frenk–White (NFW) profile suggested by the N-body simulations [18], i.e.,

$$\rho_{\text{NFW}}(r) = \frac{\rho_0}{\frac{r}{R_s} \left(1 + \frac{r}{r_s}\right)^2}. \quad (2.2)$$

The second one is the Einasto profile which gives a better fit to the simulation data than the NFW profile [19, 20]. It is given by

$$\rho_{\text{Ein}}(r) = \rho_0 \exp \left[-\frac{2}{\alpha} \left\{ \left(\frac{r}{r_s} \right)^\alpha - 1 \right\} \right]. \quad (2.3)$$

Since both the NFW and Einasto profiles are cuspy in the Galactic center, we also investigate a cored profile to see the profile dependence clearly. The third profile is the pseudo-isothermal profile (PIT) [21]

$$\rho_{\text{Iso}}(r) = \frac{\rho_0}{1 + (r/r_s)^2}. \quad (2.4)$$

Parameters used in the numerical calculation are shown in Table 1, taken from [22] for NFW and Einasto profiles, and [23] for the PIT profile. In the table, the local DM density is represented as $\rho_{\text{DM},\odot}$, and ρ_0 is normalized to reproduce that value of $\rho_{\text{DM},\odot}$.

Table 1: Parameters on DM profiles

	$\rho_{\text{DM},\odot}$ [GeV/cm ³]	ρ_0 [GeV/cm ³]	r_s [kpc]	α
NFW	0.38	0.83	11.0	-
Einasto	0.38	0.30	9.2	0.18
PIT	0.35	3.56	2.7	-

3 Numerical Result and discussion

In direct detection experiments with directional sensitivity, the energy and angle of nuclear recoil are expected to be detected. We discuss the results obtained from the simulations for each of these in this section.

3.1 Angular distribution of CR-DM and nuclear recoil

Figure 2 shows the sky maps of incoming distributions of the CR-DMs of 1 MeV mass expected at the Solar system for three density profiles assumed. The left, middle, and right figures correspond to NFW, Einasto, and PIT profiles, respectively. In the NFW and Einasto profiles, the arrival of CR-DM is highly concentrated in the direction of the Galactic center, while in the PIT case, the arrival of CR-DM is found over a wide area centered at the Galactic

center. There is almost no difference in the directional distributions of the CR-DM in the mass range between 1 keV and 1 GeV.

Next, we will move to the directional distributions of nuclear recoils by the CR-DMs. In Figures 3-5, the angular distributions of the recoiled nuclei are shown in the whole sky maps for the following reference cases:

- the targets are p , F, and Ag,
- the DM profiles are NFW, Einasto, and PIT,
- the DM masses are 0.1 GeV, 1 MeV, and 10 keV.

These figures are intended to illustrate the ideal cases without the consideration of detector response (energy threshold, energy resolution, quenching factor and others) and any types of background. Note that the center of the figures corresponds to the arrival from the direction of the Galactic center, thus in all cases, CR-DM flux from the Galactic center direction is significantly higher than the contribution from other directions. There is no noticeable difference between the NFW and Einasto cases in sky map density plots, while there is a distinct difference between the PIT case and the other two cases. In the NFW and Einasto cases, the profiles in the Galactic center are cuspy, but it is cored in the case of the PIT profile. This property is reflected in the fact that events are less dense in the Galactic center in the PIT case than in the NFW case.

3.2 Energy dependence of the angular distribution

We now discuss the distributions of recoil energy and scattering angle to see the dependence of CR-DM mass, which is not visualized in the sky maps in the previous section. Differential angular distributions expected with the p , F, and Ag targets are shown in Figure 6, 7, and 8, respectively. The rate is shown in the unit of event number per second per kilogram. NFW, Einasto and PIT cases are shown in the left, center, and right columns of each figure. Cases with the CR-DM mass of 0.1 GeV, 1 MeV, and 10 keV are shown in the top, center, and bottom rows in each figure. SI interactions with the DM are assumed for p and Ag targets, while SD interactions are assumed for F target. We assume the cross section of DM and proton interaction is $\sigma_{\chi-p} = 10^{-32} \text{ cm}^2$, for which no experimental constraint has been given yet to neither SI nor SD interactions for $m_\chi \lesssim 0.1 \text{ GeV}$ case [4]. See the Appendix for the sensitivity with the F target in the case of the SI interactions. The detector energy threshold $E_{\text{thr}} = 10 \text{ keV}$ is assumed for the p and F targets, and the threshold $E_{\text{thr}} = 100 \text{ keV}$ for the Ag target is assumed as the lower limit of the detection energy. The event rates expected in the energy range above the detector energy threshold and in which elastic scattering occurs are shown in the figures [24]. The black histograms show the distribution over the whole energy range of interest, while colored ones show the distributions corresponding to three recoil energy ranges. Note that we discarded high momentum transfer events before making these angular distributions in order to conservatively focus on the elastic scattering events in this study. The reason high momentum transfer events are not included for the analysis is that inelastic scatterings are expected to dominate once the kinetic energy of DM is high enough to see the internal structure of the nucleus. To discuss inelastic scatterings between the DM and target nuclei, we need to introduce some assumptions depending on the type of DM and its interactions [7, 25–27]. In this paper, we prefer to discuss the properties of the CR-DM in general manners as much as possible, thus we will focus only on the elastic

scatterings, which can be discussed as a more plausible approach. We assume that if the de Broglie wavelength of the DM is longer than that of the target nuclei, it can be treated as a perfect elastic scattering. For the sake of consistency and considering current detector setup, only such events are included here, i.e. events with energies above 10, 3, and 0.6 MeV are discarded for p , F, and Ag targets, respectively.

As can be easily expected, forward scattering events make peaks at $\cos \gamma_{\text{G.C.}} = 1$. Some distributions are found to have peaks in the center at $\cos \gamma_{\text{G.C.}} = 0$. These central peaks are clearly visible in the distributions for heavy CR-DMs and disappear in ones for light CR-DMs. The central peaks correspond to the case where the target and CR-DM do not change the direction of their motions from their initial ones in the center-of-mass system through the scatterings. This kind of scattering, in which the target and CR-DM graze each other in the center-of-mass system, becomes less visible in the laboratory frame as the CR-DM mass decreases. In light CR-DM case, in the center-of-mass system, the CR-DM hits a light target and both CR-DM and target are bounced away in the opposite direction from its initial state. As a result, a prominent peak is produced at $\cos \gamma_{\text{G.C.}} = 1$, which is the direction expected to be naively scattered from the Galactic center.

The energy dependence is similar for the NFW and Einasto cases. On the other hand, from the figures, it is seen that there is a difference between the PIT case and the NFW case, due to the different structures in the center of the galaxy. Now we will take a closer look at the case of the PIT profile. The central peak near $\cos \gamma_{\text{G.C.}} = 0$ is moderate and less noticeable than in the NFW and Einasto profiles. This is because the PIT profile has a core at the Galactic center, and it is clear from Figure 3-5 that the CR-DM signal comes from a wider range than that in the cases of the other two profiles in which the CR-DM comes from the very small direction of the Galactic center.

3.3 Asymmetry and sensitivity

To quantify the forward-backward asymmetries of the recoil direction distributions, a parameter A is defined as

$$A = \frac{n_+ - n_-}{n_+ + n_-}, \quad (3.1)$$

where n_+ and n_- are the number of events in $\cos \gamma_{\text{G.C.}} > 0$ and $\cos \gamma_{\text{G.C.}} < 0$, respectively.

Figures 9 show the asymmetry parameters and their errors obtained by the simulation. The colors represent the density profiles. The errors are statistical ones. The number of events is normalized as 5.0 kg-yr exposure of the nano imaging tracker (NIT) for the target p and Ag, and 155 kg-yr exposure of SF_6 gas. The latter is based on the assumption of the exposure 1000 m^3 SF_6 gas at 20 Torr and one year [14]. The weight ratios of p and Ag in the NIT are set at 1.6% and 44.5%, respectively [28]. For light CR-DMs below $O(10) - O(100)$ keV mass, enough statistics clearly confirm the directionality originated by signals coming from the Galactic center direction, since the number of events discarded is smaller than for heavy CR-DM case and the central peak disappears. As already mentioned, events with high recoil energy, which often occur in heavy CR-DM cases, are discarded because they are not elastic scattering, thus the number of events available for the analysis is reduced and the error is significant.

Figure 10 shows the evolution of the null-rejection significance of the asymmetry parameter A with each target, where the range of the exposure corresponds up to five years for the same configuration as that in Figure 9. The CR-DM masses are assumed to be 1 keV

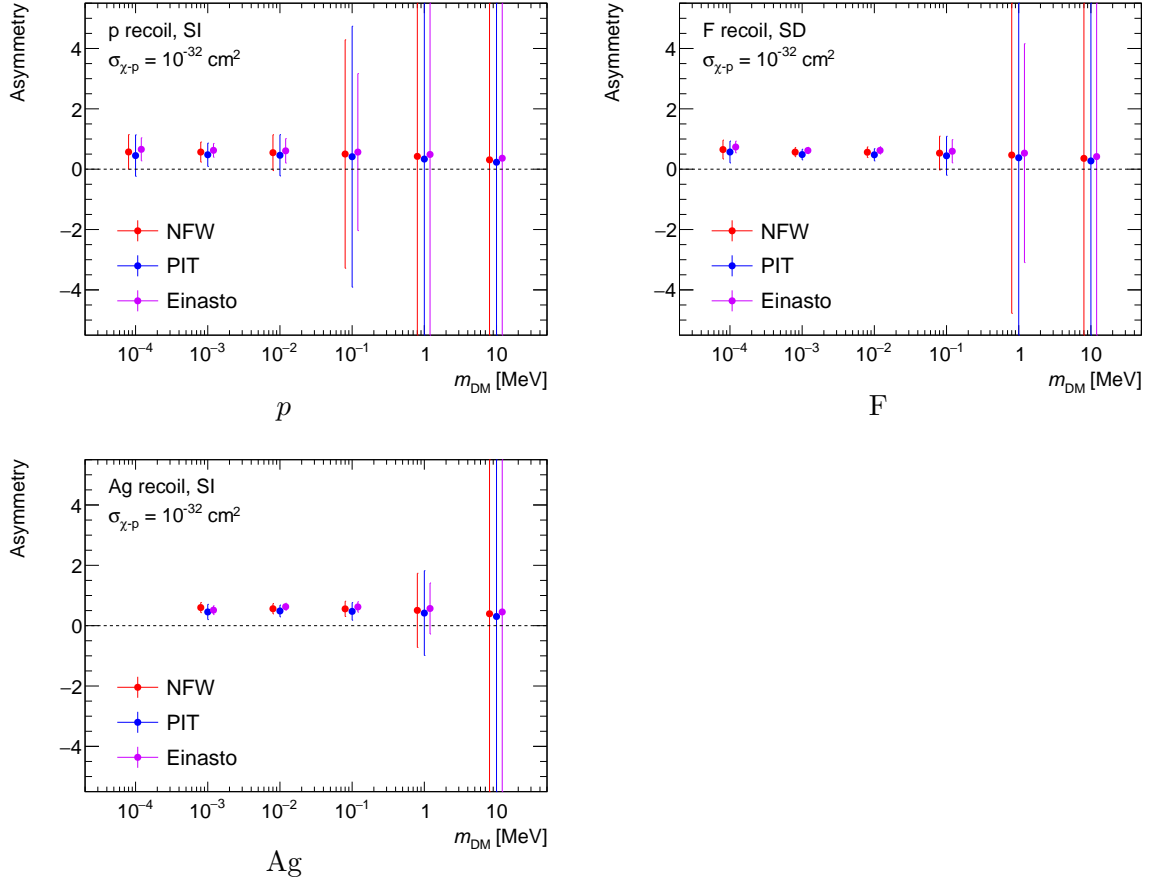


Figure 9: Simulated asymmetry for each target and CR-DM mass. Colors indicate the density profiles. Scattering cross section for DM and proton is assumed to be $\sigma_{\chi p} = 10^{-32} \text{ cm}^2$, and the exposure is assumed to be NIT 5.0 kg-yr for the target p and Ag, and SF₆ 155 kg-yr for the target F.

(dotted lines) and 100 keV (dashed lines). As can be inferred from Figures 9, assuming elastic scattering, all targets investigated have sufficient potential for the null-rejection of the asymmetry parameter A within the scope of future upgrades envisioned. With the exposure, the asymmetry can be confirmed with more than 5σ confidence level for 1 keV mass CR-DM case. For the case of SD interaction using fluorine target, the NEWAGE experiment is developing a 1 m³ scale detector filled with SF₆ gas. Further update is planned as CYGNUS-1000 experiment [14] which has 1000 m³ scale gaseous time projection chamber (TPC). It will achieve 5σ sensitivity for the 1 keV CR-DM mass by 2.5 years' measurement. For the NEWSdm experiment, the device production system at the Gran Sasso National Laboratory (LNGS) has been operated, and it is possible to produce the 10 kg scale target with the current system. In addition, the new scanning systems with 0.5 kg/year/machine are being developed, and several kg-scale scanning will be achieved by the same upgrade of existing five machines. Further high scanning speed machine with $> 5 \text{ kg/year/machine}$ has already been designed by wide field of views with multi-camera imaging and optimal driving motion system. By that, several 10 kg scale experiment will be achieved. Low energy threshold tracking will be achieved by the finer grain nuclear emulsions [28] and super-resolution tech-

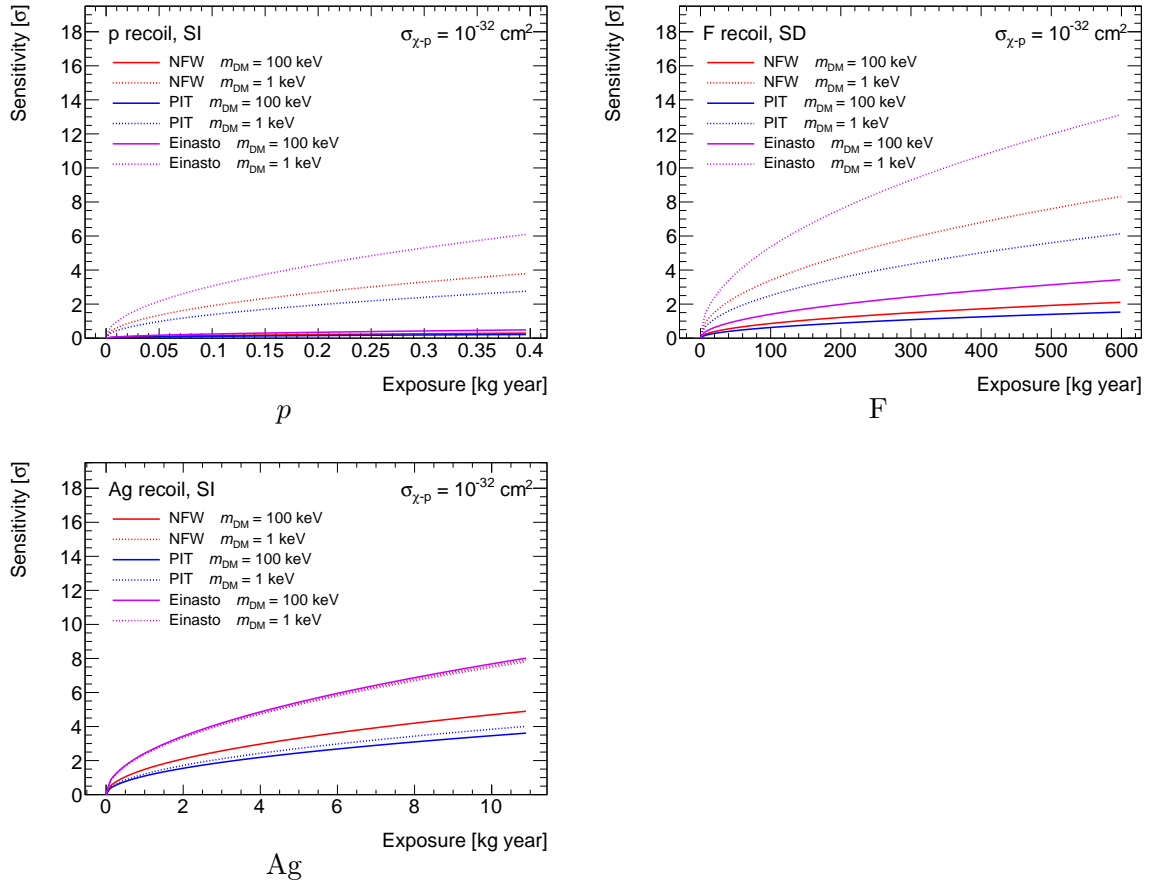


Figure 10: Null-rejection significance of the asymmetry parameter A for each target. The CR-DM masses are assumed to be 1 keV and 100 keV, and are marked with dotted and solid lines, respectively. Scattering cross section for DM and proton is assumed to be $\sigma_{\chi p} = 10^{-32} \text{ cm}^2$, same as the previous figures.

niques [29]. Therefore, taking into account the possibility of future upgrades, both NEWAGE and NEWSdm would have the potential to verify the light CR-DM arriving from the direction of the Galactic center.

4 Conclusion

Up-scattering of DM by cosmic-rays is an undeniable key phenomenon that can allow the search for light DMs, which are not easy to reach by standard nuclear recoil methods. The CR-DMs are expected to arrive mostly from the direction of the Galactic center, where the density of the DM is high, and thus can be examined with direction-sensitive detectors. In this paper, we study the detection possibilities of CR-DMs with directional detectors and investigate the expected energy and angular distributions.

We find that almost independent of the DM density profiles, CR-DM tends to come from the direction of the Galactic center, and the targets in the detector are scattered towards the forward direction. Assuming elastic scattering of DM and target, we also investigate the sensitivity of directional detectors to verify the existence of CR-DM. Our study showed that

the asymmetry of nuclear recoil is expected to hold the characteristic signature of the CR-DM. It is shown that the feature can be verified by directional detectors, especially for light DM with mass below $O(100) - O(10)$ keV. With scattering cross section of DM and proton as $\sigma_{\chi-p} = 10^{-32} \text{ cm}^2$ and $m_\chi = 1 \text{ keV}$, the asymmetry can be evaluated at 6σ , 13σ , and 8σ for the p target (the SI interaction), for the F target (the SD interaction), and for the Ag target (the SI interaction), respectively. For the evaluation, exposures 0.4 kg-yr, 600 kg-yr, and 11 kg-yr are assumed for p , F, and Ag targets, respectively. These large exposure can be achieved with future large detectors like CYGNUS and NEWSdm.

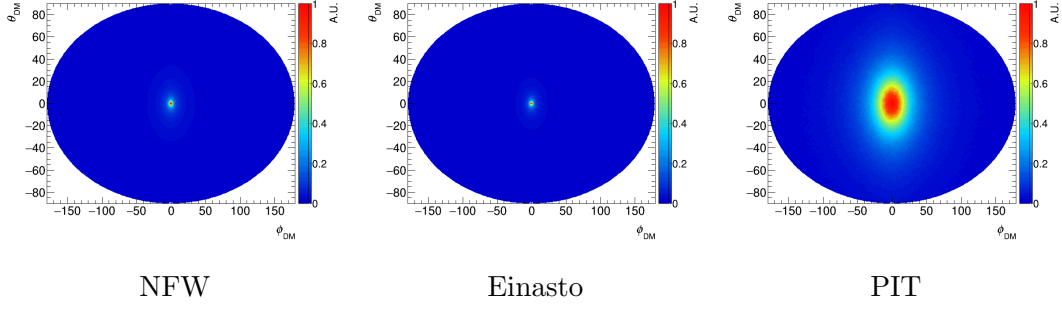


Figure 2: Sky map of the CR-DM in the Solar system. The left-handed side, the center, and the right-handed side correspond to the NFW, the Einasto, and the PIT profile, respectively. The CR-DM mass is 1 MeV. Density of the number of events is shown by arbitrary units (A.U.).

Acknowledgments

It is a pleasure to thank S. Matsumoto, K. Hata, K. Hayashi, C. Cappiello and H. Oshima for helpful discussions. KIN is also grateful to S. Kime, T. Tomiya and N. Ikeda for discussion on the early stages of this work. This work was supported by JSPS KAKENHI Grant Number 19H05806, 26104005, (A) 16H02189, (A) 18H03699, (C) 21K03562, (C) 21K03583, 21K13943, 22H04574 and Wesco Scientific Promotion Foundation.

References

- [1] E. Aprile, et al. Dark Matter Search Results from a One Ton-Year Exposure of XENON1T. *Phys. Rev. Lett.*, Vol. 121, No. 11, p. 111302, 2018.
- [2] J. Aalbers, et al. First Dark Matter Search Results from the LUX-ZEPLIN (LZ) Experiment. 7 2022.
- [3] Christopher V. Cappiello, Kenny C. Y. Ng, and John F. Beacom. Reverse Direct Detection: Cosmic Ray Scattering With Light Dark Matter. *Phys. Rev. D*, Vol. 99, No. 6, p. 063004, 2019.
- [4] Torsten Bringmann and Maxim Pospelov. Novel direct detection constraints on light dark matter. *Phys. Rev. Lett.*, Vol. 122, No. 17, p. 171801, 2019.
- [5] Yohei Ema, Filippo Sala, and Ryosuke Sato. Light Dark Matter at Neutrino Experiments. *Phys. Rev. Lett.*, Vol. 122, No. 18, p. 181802, 2019.
- [6] Shao-Feng Ge, Jianglai Liu, Qiang Yuan, and Ning Zhou. Diurnal Effect of Sub-GeV Dark Matter Boosted by Cosmic Rays. *Phys. Rev. Lett.*, Vol. 126, No. 9, p. 091804, 2021.
- [7] Gang Guo, Yue-Lin Sming Tsai, Meng-Ru Wu, and Qiang Yuan. Elastic and Inelastic Scattering of Cosmic-Rays on Sub-GeV Dark Matter. *Phys. Rev. D*, Vol. 102, No. 10, p. 103004, 2020.
- [8] Nicole F. Bell, James B. Dent, Bhaskar Dutta, Sumit Ghosh, Jason Kumar, Jayden L. Newstead, and Ian M. Shoemaker. Cosmic-ray upscattered inelastic dark matter. *Phys. Rev. D*, Vol. 104, p. 076020, 2021.
- [9] Jie-Cheng Feng, Xian-Wei Kang, Chih-Ting Lu, Yue-Lin Sming Tsai, and Feng-Shou Zhang. Revising inelastic dark matter direct detection by including the cosmic ray acceleration. *JHEP*, Vol. 04, p. 080, 2022.

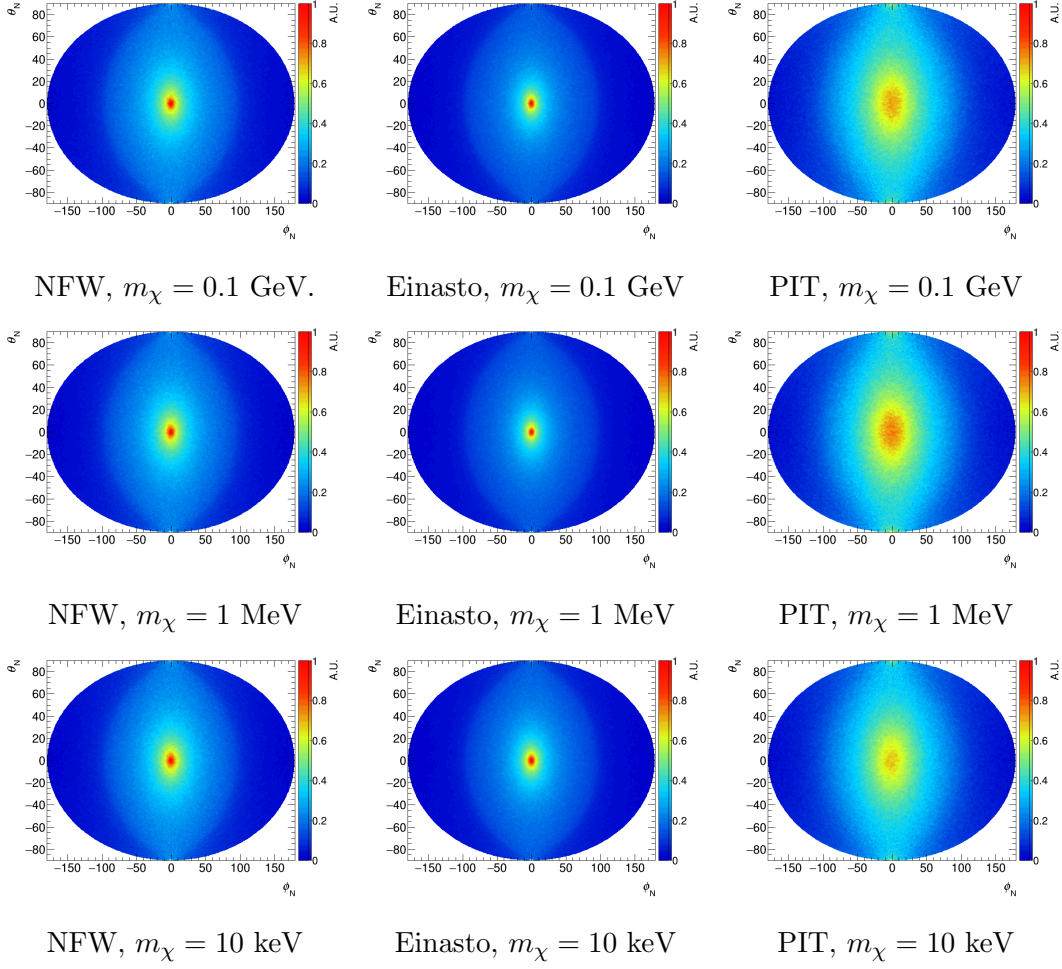


Figure 3: Sky map of the nuclear recoil directions in the Solar system. The left-handed side, the center, and the right-handed side correspond to the NFW, the Einasto, and the PIT profile, respectively. The upper column corresponds to the CR-DM mass of 0.1 GeV, the middle column to 1 MeV, and the lower column to 10 keV. The target is p . The SI interaction of DM and target is assumed.

- [10] K. Abe, et al. Search for Cosmic-ray Boosted Sub-GeV Dark Matter using Recoil Protons at Super-Kamiokande. 9 2022.
- [11] Debjyoti Bardhan, Supritha Bhowmick, Diptimoy Ghosh, Atanu Guha, and Divya Sachdeva. Boosting through the Darkness : Bounds on boosted dark matter from direct detection. 8 2022.
- [12] James Alvey, Torsten Bringmann, and Helena Kolesova. No room to hide: implications of cosmic-ray upscattering for GeV-scale dark matter. 9 2022.
- [13] F. Mayet, et al. A review of the discovery reach of directional Dark Matter detection. *Phys. Rept.*, Vol. 627, pp. 1–49, 2016.
- [14] S. E. Vahsen, et al. CYGNUS: Feasibility of a nuclear recoil observatory with directional sensitivity to dark matter and neutrinos, arXiv:2008.12587. 8 2020.
- [15] A. Aleksandrov, et al. NEWS: Nuclear Emulsions for WIMP Search. 4 2016.
- [16] N. Agafonova, et al. Discovery potential for directional Dark Matter detection with nuclear

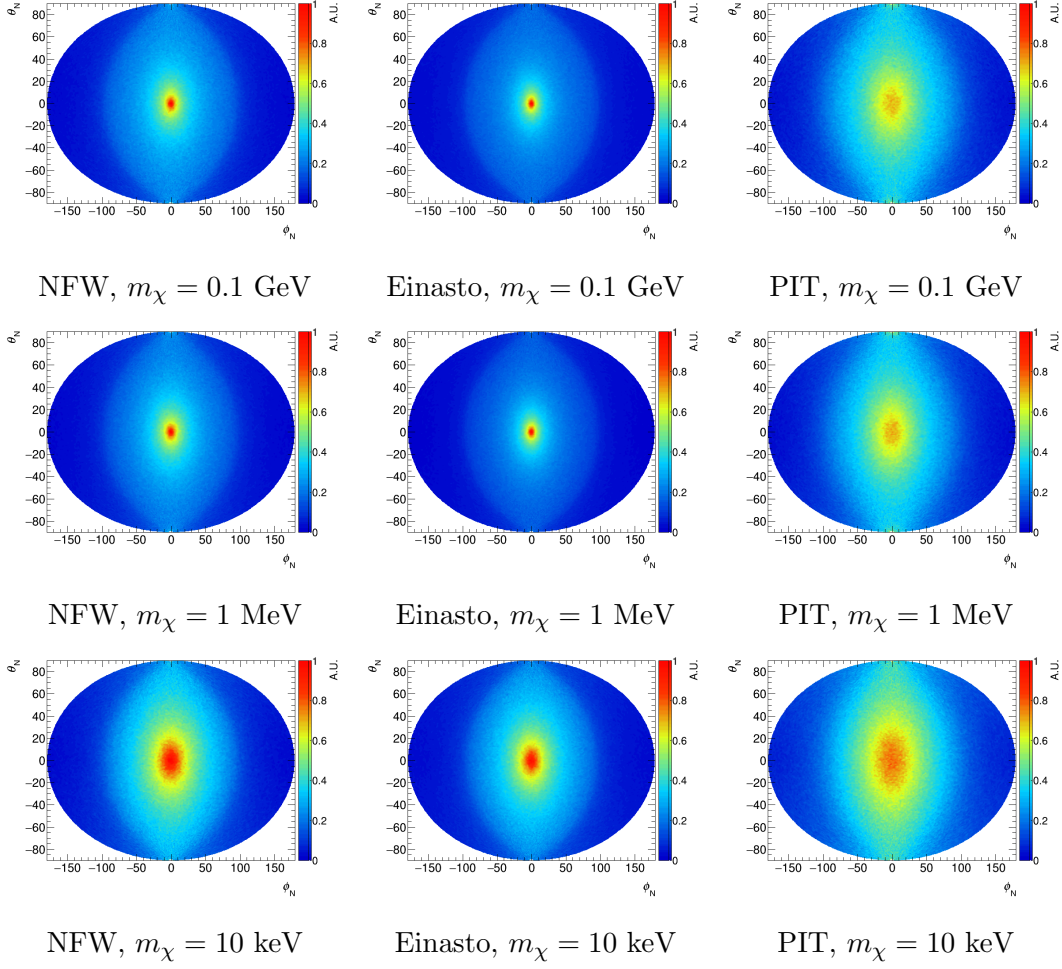


Figure 4: Legend is same as Figure 3 except that the target atom in the direct detection is F.

- emulsions. *Eur. Phys. J. C*, Vol. 78, No. 7, p. 578, 2018.
- [17] A.E. Vladimirov, S.W. Digel, G. Jóhannesson, P.F. Michelson, I.V. Moskalenko, P.L. Nolan, E. Orlando, T.A. Porter, and A.W. Strong. Galprop webrun: An internet-based service for calculating galactic cosmic ray propagation and associated photon emissions. *Computer Physics Communications*, Vol. 182, No. 5, p. 1156–1161, May 2011.
 - [18] Julio F. Navarro, Carlos S. Frenk, and Simon D. M. White. A Universal density profile from hierarchical clustering. *Astrophys. J.*, Vol. 490, pp. 493–508, 1997.
 - [19] J. F. Navarro, E. Hayashi, C. Power, A. R. Jenkins, C. S. Frenk, S. D. M. White, V. Springel, J. Stadel, and T. R. Quinn. The inner structure of λ cdm haloes - iii. universality and asymptotic slopes. *Monthly Notices of the Royal Astronomical Society*, Vol. 349, No. 3, p. 1039–1051, Apr 2004.
 - [20] Alister W. Graham, David Merritt, Ben Moore, Jürg Diemand, and Balša Terzić. Empirical models for dark matter halos. ii. inner profile slopes, dynamical profiles, and ρ/σ^3 . *The Astronomical Journal*, Vol. 132, No. 6, p. 2701–2710, Jan 2006.
 - [21] Raul Jimenez, Licia Verde, and S. Peng Oh. Dark halo properties from rotation curves. *Mon. Not. Roy. Astron. Soc.*, Vol. 339, p. 243, 2003.

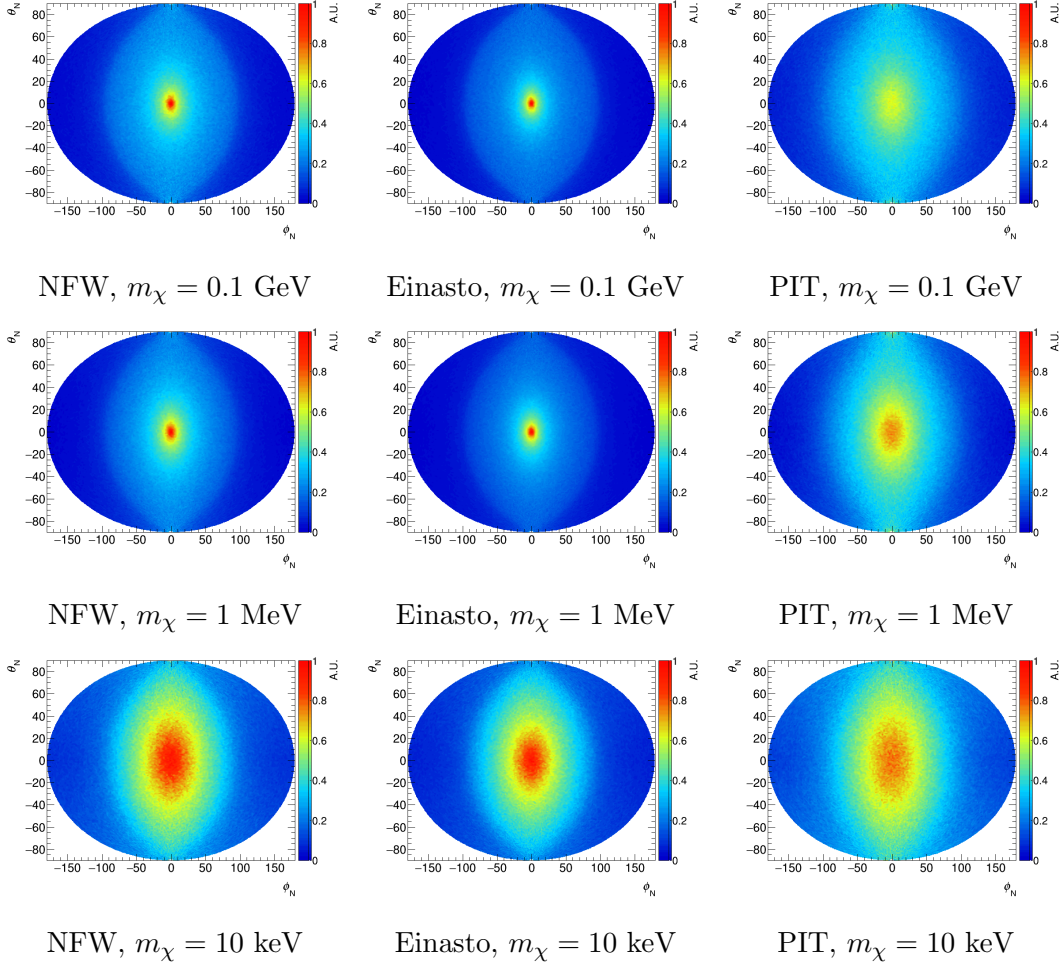


Figure 5: Legend is same as Figure 3 except that the target atom in the direct detection is Ag.

- [22] P.F. de Salas, K. Malhan, K. Freese, K. Hattori, and M. Valluri. On the estimation of the local dark matter density using the rotation curve of the milky way. *Journal of Cosmology and Astroparticle Physics*, Vol. 2019, No. 10, pp. 037–037, oct 2019.
- [23] Christopher Wegg, Ortwin Gerhard, and Marie Bieth. The gravitational force field of the galaxy measured from the kinematics of RR lyrae in gaia. *Monthly Notices of the Royal Astronomical Society*, Vol. 485, No. 3, pp. 3296–3316, feb 2019.
- [24] T. Ikeda, T. Shimada, H. Ishiura, K.D. Nakamura, T. Nakamura, and K. Miuchi. Development of a negative ion micro tpc detector with sf6 gas for the directional dark matter search. *Journal of Instrumentation*, Vol. 15, No. 07, p. P07015, jul 2020.
- [25] John R. Ellis, R. A. Flores, and J. D. Lewin. Rates for Inelastic Nuclear Excitation by Dark Matter Particles. *Phys. Lett. B*, Vol. 212, pp. 375–380, 1988.
- [26] J. Engel and P. Vogel. Neutralino inelastic scattering with subsequent detection of nuclear gamma-rays. *Phys. Rev. D*, Vol. 61, p. 063503, 2000.
- [27] G. Arcadi, C. Döring, C. Hasterok, and S. Vogl. Inelastic dark matter nucleus scattering. *JCAP*, Vol. 12, p. 053, 2019.

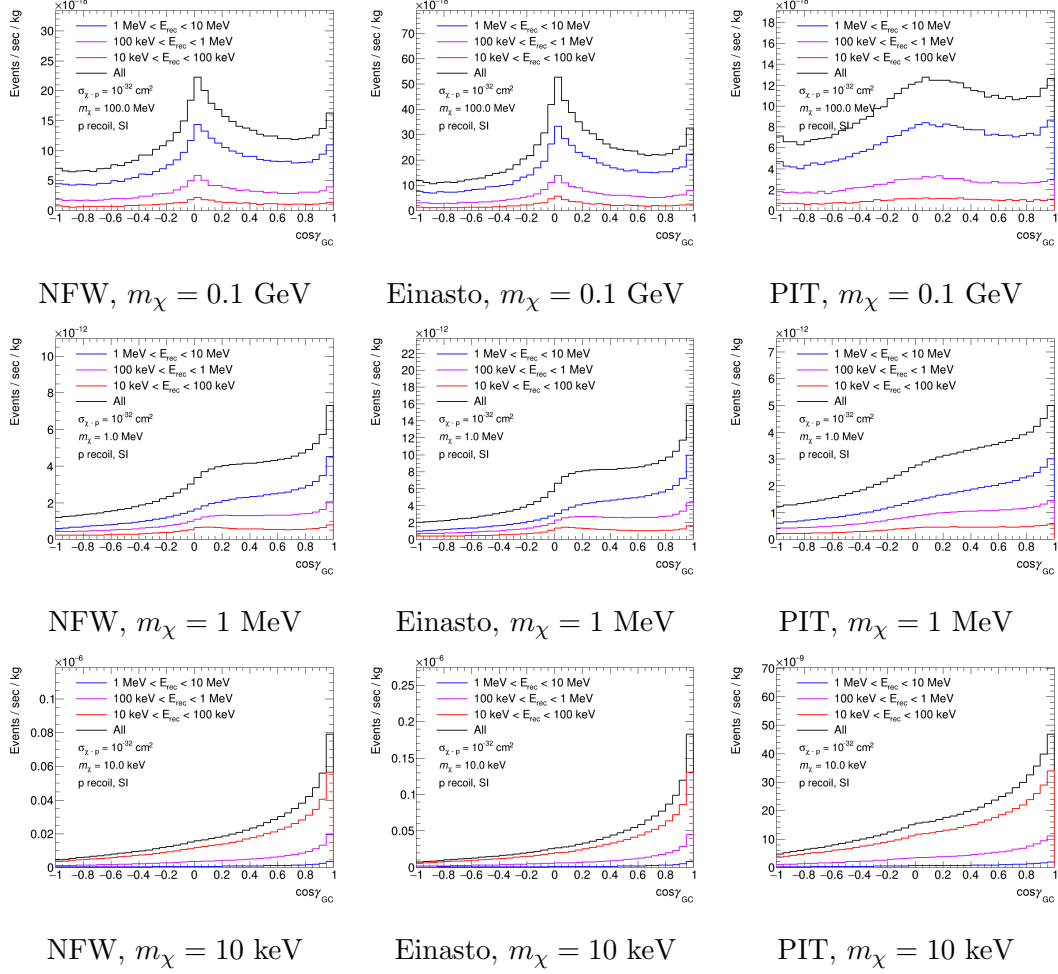


Figure 6: Angular distribution of nuclear recoil in each energy band, in the Solar system. The left-handed side, the center, and the right-handed side correspond to the NFW, the Einasto, and the PIT profile, respectively. The upper column corresponds to the CR-DM mass of 1 GeV, the middle column to 1 MeV, and the lower column to 10 keV. The target is p . The SI interaction of DM and target is assumed.

- [28] Takashi Asada, Tatsuhiro Naka, Ken-ichi Kuwabara, and Masahiro Yoshimoto. The development of a super-fine-grained nuclear emulsion. *PTEP*, Vol. 2017, No. 6, p. 063H01, 2017.
- [29] Andrey Alexandrov, Takashi Asada, Di Crescenzo Antonia De Lellis, Giovanni, Valerio Gentile Gentile, Tatsuhiro Naka, Valeri Tioukov, and Atsuhiko Umemoto. Super-resolution high-speed optical microscopy for fully automated readout of metallic nanoparticles and nanostructures. *Sci. Rep.*, Vol. 10, No. 18773, 2020.

A The SI and SD cross section

Fluorine is the target assumed in the directional direct detection through SD interactions. The sensitivity to SI and SD cross sections varies by a factor $\eta_A = \sigma_{\chi-p}^{\text{SI}}/\sigma_{\chi-p}^{\text{SD}}$. By evaluating

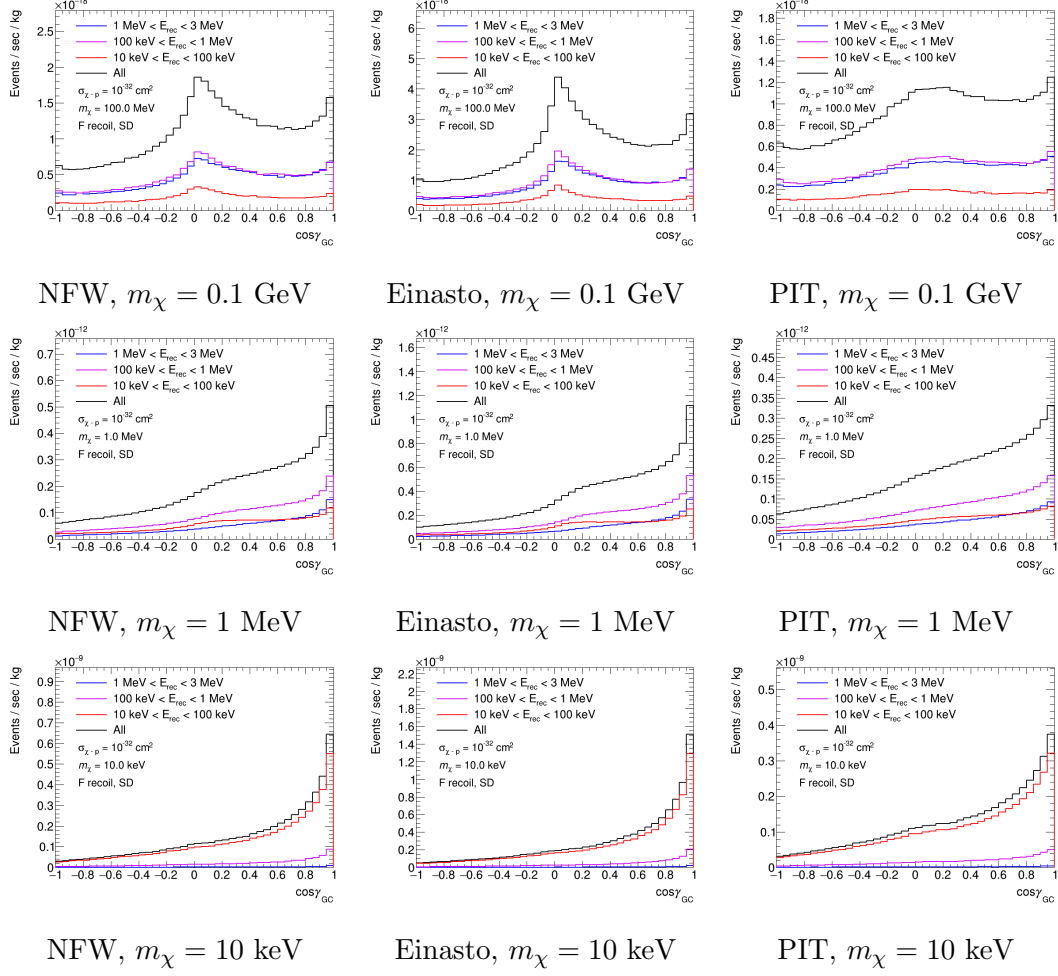


Figure 7: Legend is same as Figure 6 except that the target atom in the direct detection is F.

the factor, the sensitivity to SD interactions in Section 3.2 can be scaled to that to SI interactions. The cross sections of DM and nucleus scattering for the SI and SD interactions $\sigma_{\chi-N}^{\text{SI,SD}}$ are

$$\sigma_{\chi-N}^{\text{SI}} = \sigma_{\chi-p}^{\text{SI}} \frac{\mu_{\chi-N}^2}{\mu_{\chi-p}^2} A^2 [\text{cm}^2], \quad (\text{A.1})$$

$$\sigma_{\chi-N}^{\text{SD}} = \sigma_{\chi-p}^{\text{SD}} \frac{\mu_{\chi-N}^2}{\mu_{\chi-p}^2} \frac{\lambda^2 J(J+1)}{0.75} [\text{cm}^2], \quad (\text{A.2})$$

respectively, where $\sigma_{\chi-p}^{\text{SD,SI}}$ is the DM and proton scattering cross section, $\mu_{\chi-N(p)}$ is the reduced mass of CR-DM and nucleus (proton), A is mass number, and $\lambda J(J+1) = 0.647$ for F. Therefore, the ratio of event number required to reach the same cross section $\sigma_{\chi-p}$, which

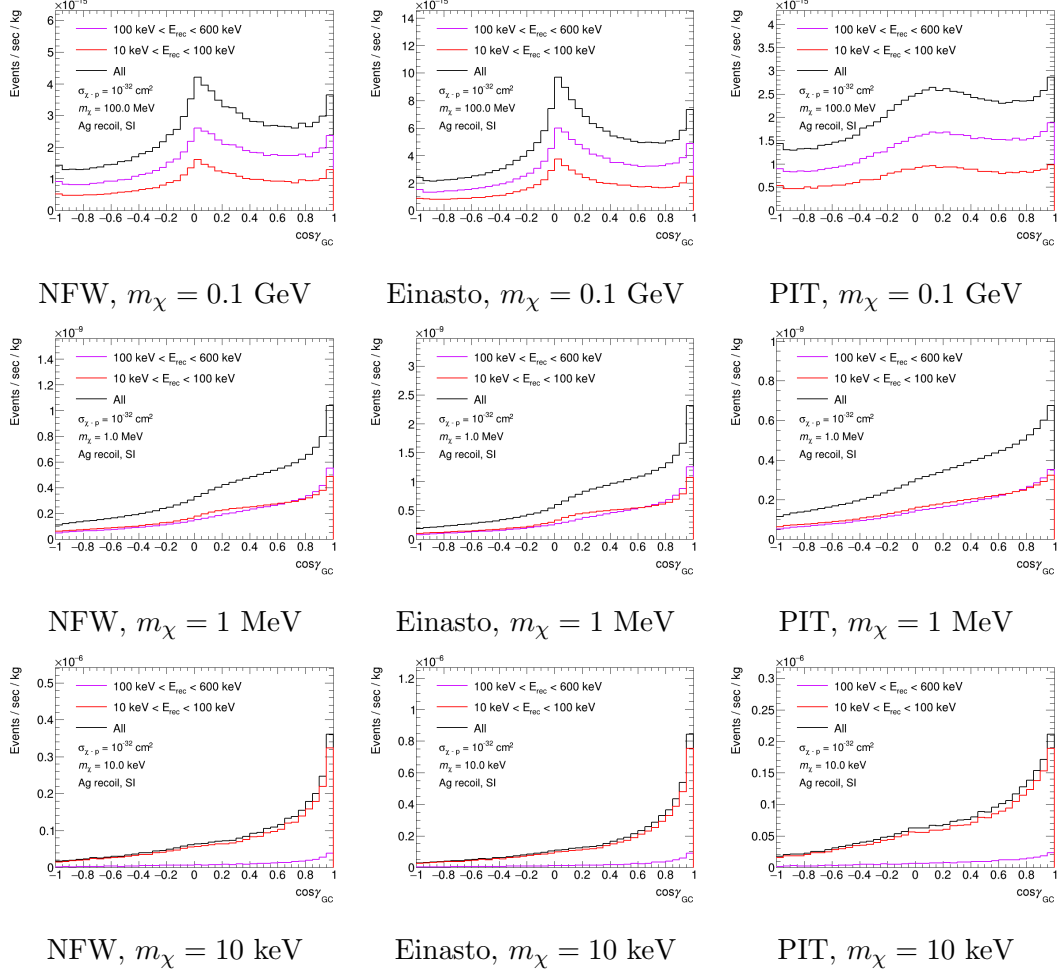


Figure 8: Legend is same as Figure 6 except that the target atom in the direct detection is Ag.

is also denoted as $\eta_A = n_{\text{SI}}/n_{\text{SD}}$, is estimated as

$$\eta_A = \frac{0.75 A^2}{\lambda^2 J(J+1)} \simeq 418. \quad (\text{A.3})$$